Eksplorium
Volume 46 No. 1, May 2025: 1–14

p-ISSN 0854-1418
e-ISSN 2503-426X

Lithological Discrimination Based on Radiometric Data: Case Study of Rabau Sector, West Kalimantan and Salumati Sector, West Sulawesi

Muhammad Wira Maulana[1], Roni Cahya Ciputra[2,*], Iskandarsyah[1], Tyto Baskara Adimedha[2], I Gde Sukadana[2], Frederikus Dian Indrastomo[2], Heri Syaeful[2], Fadiah Pratiwi[2], Yoshi Rachael[2], Faneza Nur Mardania[1], Dhatu Kamajati[3], Putri Rahmawati[3], Mirna Berliana Garwan[4]

[1]Department of Geoscience, Faculty of Mathematics and Natural Sciences, Universitas Indonesia,
Prof. Dr. Mahar Mardjono St., Building A, Depok, 16424, Indonesia
[2]Research Center for Nuclear Material and Radioactive Waste Technology,
Research Organization for Nuclear Energy, National Research and Innovation Agency (BRIN)
B.J. Habibie Science and Technology Park, Tangerang Selatan, Banten 15314, Indonesia
[3]Bureau for Public Communication, General Affairs, and Secretariat,
Executive Secretariat, National Research and Innovation Agency (BRIN),
B.J. Habibie Administrative Park, Jakarta, 10340, Indonesia
[4]Directorate for Laboratory Management, Research Facilities and Science and Technology Park,
Deputy for Research and Innovation Infrastructure, National Research and Innovation Agency (BRIN),
B.J. Habibie Administrative Park, Jakarta, 10340, Indonesia
*E-mail: roni010@brin.go.id

Article received: 3 April 2025, revised: 10 May, accepted: 31 May 2025
DOI: 10.55981/eksplorium.2025.11475

ABSTRACT

This study evaluates the applicability of radiometric methods for lithological discrimination in tropical environments, with a focus on two uranium exploration sites in Indonesia: the Rabau Sector in West Kalimantan and the Salumati Sector in West Sulawesi. These locations were selected to represent various lithologies within the uranium exploration program. The aim is to determine whether gamma-ray spectrometry, commonly effective in arid environments, can also delineate lithological boundaries and alteration zones under conditions of intense weathering and dense vegetation cover of tropical area. Ground-based radiometric data were collected using the RS-125 gamma spectrometer to record the concentration of potassium (K), equivalent uranium (eU), and equivalent thorium (eTh). Data processing involved anisotropy analysis, geostatistical interpolation using ordinary kriging, ternary RGB composite mapping, and delineation of radiometric domains. The resulting radiometric maps were then qualitatively compared with existing geological maps for validation. The results show that radiometric signatures, particularly eTh and eU, can effectively distinguish rock units with differing genesis or degrees of alteration, despite tropical conditions. In Rabau, where lithologies share a common protolith, elevated eU concentrations correspond to hornfels, while metatuff and metasiltstone remain indistinguishable, indicating the influence of thermal metamorphism on radiometric responses. In Salumati, eTh and eU zoning within phonolite suggest compositional variability or differential alteration, and elevated eU in altered tuff reflects uranium remobilization in smectite-rich zones. These findings demonstrate that, despite the challenges posed by tropical climates, radiometric mapping remains a viable tool for lithological discrimination and early-stage uranium exploration in Indonesia. This work extends the application of radiometric techniques beyond arid environments and underscores the need to integrate radiometric interpretation with genetic, provenance, and alteration context in tropical geological mapping.

Keywords: Rabau, Salumati, lithological discrimination, radiometric method, geostatistics

INTRODUCTION

Radiometric surveying enables the mapping of radionuclide distribution, typically potassium (K), uranium (U), and thorium (Th), by detecting the gamma radiation emitted during their natural decay at the Earth's surface. Multispectral gamma spectrometry, which exploits the characteristic energy windows of each radionuclide, allows quantitative determination of their concentration. Geologists have long employed this method to characterize lithological units with varying radioelement content, making it a valuable tool in the early stages of mineral exploration to distinguish rock units that are prospective for, or host to, mineralization [1]. Airborne deployment further extends its coverage, enabling investigation of otherwise inaccessible terrain [2]–[4]. Numerous studies and applications have demonstrated its advantages in understanding the geological heterogeneity, including sedimentary environments analysis [5], [6], volcanic rocks characterization [7], [8], mapping hydrothermal alteration [7]–[10], and distinguishing vein from host rocks in epithermal gold mineralization [11].

Most documented applications have been conducted in arid regions with sparse vegetation, where surface conditions favor gamma-ray detection. In contrast, tropical settings present additional challenges, including deep weathering profiles and dense vegetation cover, which attenuate the gamma signal. The radiometric methods have the potential to support geologic mapping under these conditions. In Indonesia, radiometric surveys have primarily targeted radioactive mineral exploration by identifying radiometric anomalies linked to mineral occurrences. For example, surveys in Mamuju, West Sulawesi, delineated variations in U and Th concentrations in soils and rocks, which in turn corresponded to rock-type distribution and radioelement anomalies [12], [13]. Similarly, mapping in Bangka hinted at its capacity for lithological discrimination [14], [15]. Nonetheless, these studies did not explicitly assess its effectiveness in highly weathered, tropical terrains. This gap in methodology underpins the present study, which aims to evaluate the capability of radiometric techniques for lithological discrimination in such environments.

Two case study areas were selected: the Rabau Sector in Melawi Regency, West Kalimantan, and the Salumati Sector in Mamuju, West Sulawesi, both located within the uranium exploration region. The Rabau Sector lies within the Kalan area of the Northern Zone of the Schwaner Mountains [16], [17]. The regional geology of Kalan is related to the intrusion of the Late Cretaceous Sepauk Tonalite and Sukadana Granite, leading to the metamorphism of the intruded volcanic protolith of Pinoh Metamorphic Rocks [17]–[19]. The Rabau Sector itself is located in the central area among the Kalan uranium sectors [20]. The area is composed of metasiltstone, feldspathic metatuff, and hornfels. The metasiltstone, often described as fine-grained quartzite microbiotite, hosts thin uranium-bearing veins [21]–[23] (Figure 1).

The Salumati Sector lies in the Adang volcanic complex, where volcanogenic U–Th mineralization occurs in post-collisional alkaline volcanic rocks showing both subduction-related signatures and evidence of magma mixing [16], [24]–[26]. Mamuju is located in the Adang volcanic complex, composed of post-collisional alkaline volcanic rocks, which also have a subduction signature and advanced magma mixing [27]–[30]. Morphologically, Mamuju encompasses volcanic features from the Ampalas, Mamuju, Takandeang, Sumare, and Tapalang volcanic

p-ISSN 0854-1418
e-ISSN 2503-426X

centers [26], [31], [32]. Previous work indicates that rock type and U–Th anomalies in radiometric data are influenced by hydrothermal alteration, with uranium showing mobility (e.g., adsorption onto clay-rich rocks) while thorium remains relatively immobile [12], [13]. The Salumati Sector is situated in the central part of the Tapalang volcanic complex. Its lithology is composed of phonolite, tuff lapilli, calcareous sandstone, limestone, and alluvial [33] (Figure 2).

Both sectors are lithologically diverse, making them suitable for evaluating radiometric lithological discrimination in tropical conditions. This study utilized ground-based radiometric measurements, applied geostatistical modeling to map radionuclide distributions, and conducted spatial comparisons with existing geological maps. The outcomes are intended to inform the applicability and limitations of radiometric methods as a complementary tool for geological mapping in highly weathered, tropical terrains.

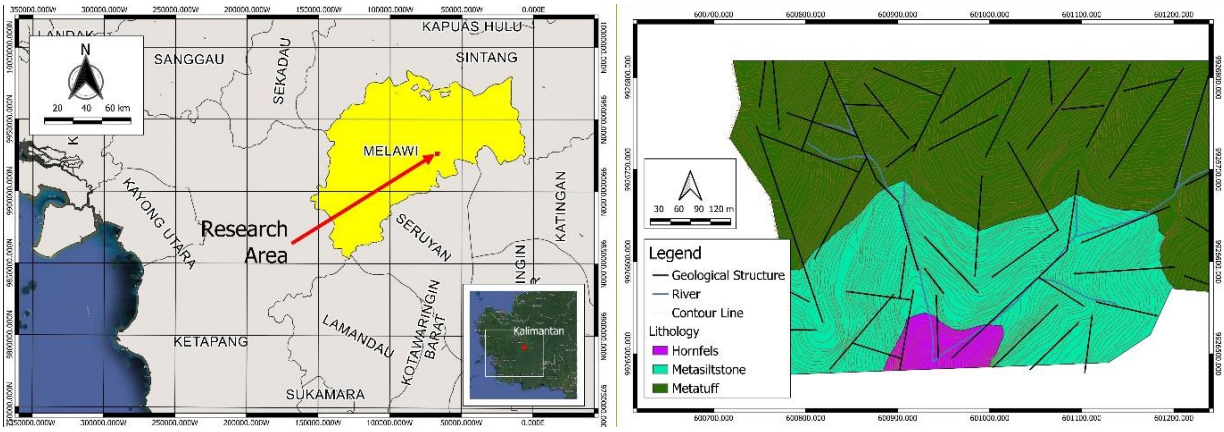

(a) **(b)**

Figure 1. Location of Rabau Sector (a) and the geological map of Rabau Sector (b)

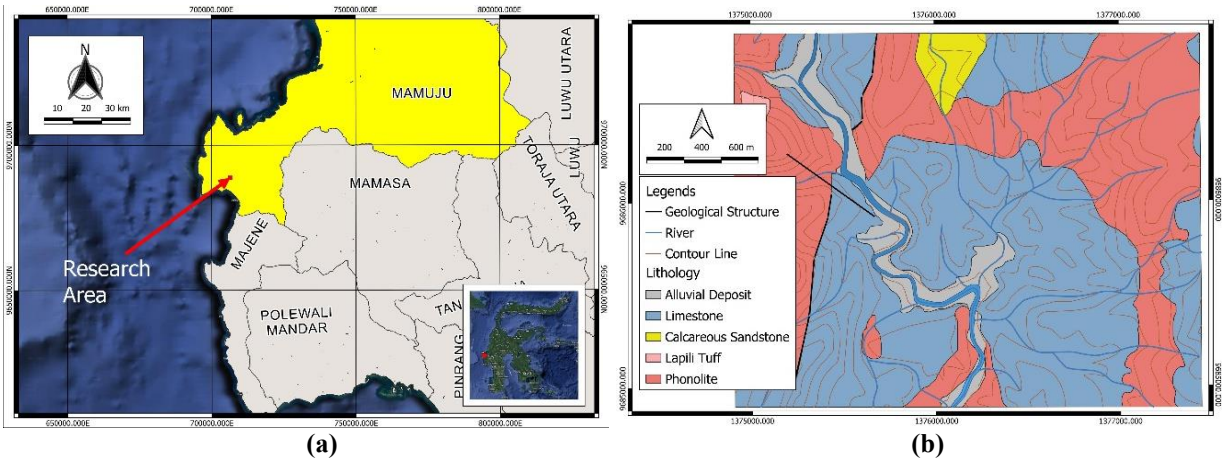

(a) **(b)**

Figure 2. Location of Salumati Sector (a) and the geological map of Salumati Sector (b)

METHODOLOGY

In this research, ground-based radiometric measurement data were acquired using an RS-125 gamma-ray spectrometer. The instrument was carried by an operator on foot, continuously recording natural gamma-ray emissions at 20-second intervals. The recorded parameters included potassium (K, in percent),

equivalent-U (eU, ppm), equivalent-Th (eTh, ppm), and gamma dose rate in micro-Sievert per hour (μSv/h). For this research, the radionuclide parameters K, eU, and eTh were used. Measurement lines were conducted as systematically as possible, with adjustments made to accommodate the local terrain to ensure coverage of the entire area of interest. A total of 3,837 measurements were collected in the Rabau Sector and 10,140 in the Salumati Sector, each within a single continuous survey period for the respective location. The spatial data distribution is presented in Figure 3. No top-cutting or data truncation was applied, ensuring that all high-value measurements were retained for further analysis.

The two-dimensional distribution of the radionuclides was modeled using the geostatistical Ordinary Kriging (OK) method. This process involved preliminary statistical analysis, variogram analysis, and variogram modeling before OK estimation. The estimated radionuclide distributions were validated using the Mean Standardized Error and Root Mean Squared Standardized Error. All spatial analyses were conducted using ArcGIS ver 10.8 software, licensed to PTBGN BATAN. The resulting radionuclide distribution maps were integrated into a composite RGB image using QGIS ver.3.40.7 software to enable simultaneous visualization of the three radio nuclides. The composites were subsequently subdivided into distinct units based on color combinations, with gradational boundaries assigned to the dominant color. Finally, the interpreted units were compared with existing geological maps for each study area using a qualitative visual assessment.

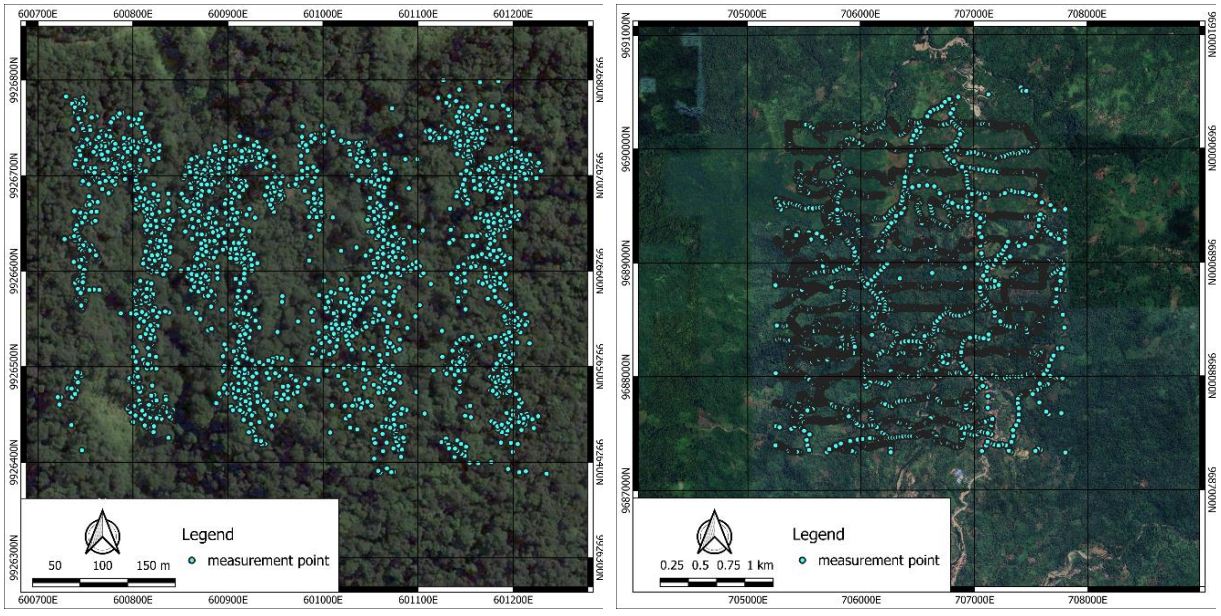

(a) **(b)**

Figure 3. Radiometric data distribution of Rabau Sector (a) and Salumati Sector (b)

RESULTS

Variogram

Variogram analysis revealed clear anisotropic patterns in the spatial distribution of radionuclides. In the Rabau Sector, potassium (K) and equivalent thorium (eTh) exhibited an NNW–SSE anisotropy, whereas equivalent uranium (eU) displayed a NE–SW anisotropy (Figure 4a-c). In the Salumati Sector, both K and eTh showed a consistent N–S anisotropy, while eU maintained the NE–SW orientation (Figure 4d-f). For parameters

p-ISSN 0854-1418
e-ISSN 2503-426X

with well-defined variogram structures, appropriate lag distances and numbers of lags were selected to optimize model fitting. The spatial dependence of these parameters was represented using spherical and nested spherical variogram models, chosen to match the observed patterns and trends (Table 1 and Figure 5).

Model validation demonstrated strong agreement with the observed data, as evidenced by mean standardized error values approaching zero and root mean squared standardized errors near unity (Table 2). The resulting spatial distribution models are presented in Figure 6 for the Rabau Sector and Figure 7 for the Salumati Sector. Classification was performed using the natural breaks method to minimize within-class variance while maximizing between-class variance.

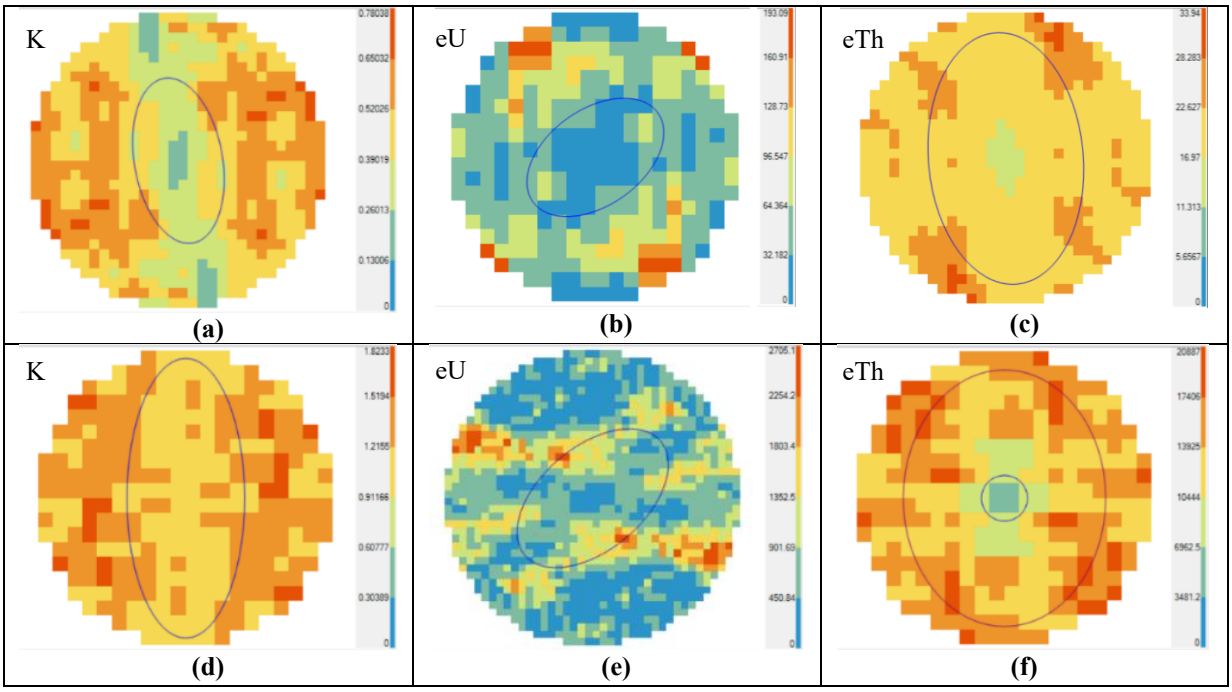

Figure 4. Variogram maps and the anisotropy interpretation of radiometric data in Rabau Sector (a-c) and Salumati Sector (d-f)

Table 1. Variogram model of radionuclide data

Sector	Parameters	Nugget Effect (10^{-4} for K and (ppm)² for eU and eTh)	Sill (C) (10^{-4} for K and (ppm)² for eU and eTh)		Nuget-sill ratio	Range (a) (meters)			
						a_1		a_2	
			C_1	C_2		Major	Minor	Major	Minor
Rabau	K (%)	0.155	0.29	-	0.348	170	90	-	-
	eU (ppm)	11	30	-	0.268	160	100	-	-
	eTh (ppm)	13	9.5	-	0.577	130	80	-	-
Salumati	K (%)	0.9	0.4	-	0.692	950	400	-	-
	eU (ppm)	100	775	-	0.114	60	35	-	-
	eTh (ppm)	565	5400	9650	0.036	125	-	700	550

In the Rabau Sector, K and eTh displayed relatively uniform spatial distributions, whereas eU was concentrated predominantly in the southern area. In the Salumati Sector, K

exhibited a pronounced N–S anisotropy, with elevated values aligned along the eastern part. Equivalent uranium showed a broad spatial range, with high concentrations in the west, while eTh values were elevated in the southern and central parts of the sector.

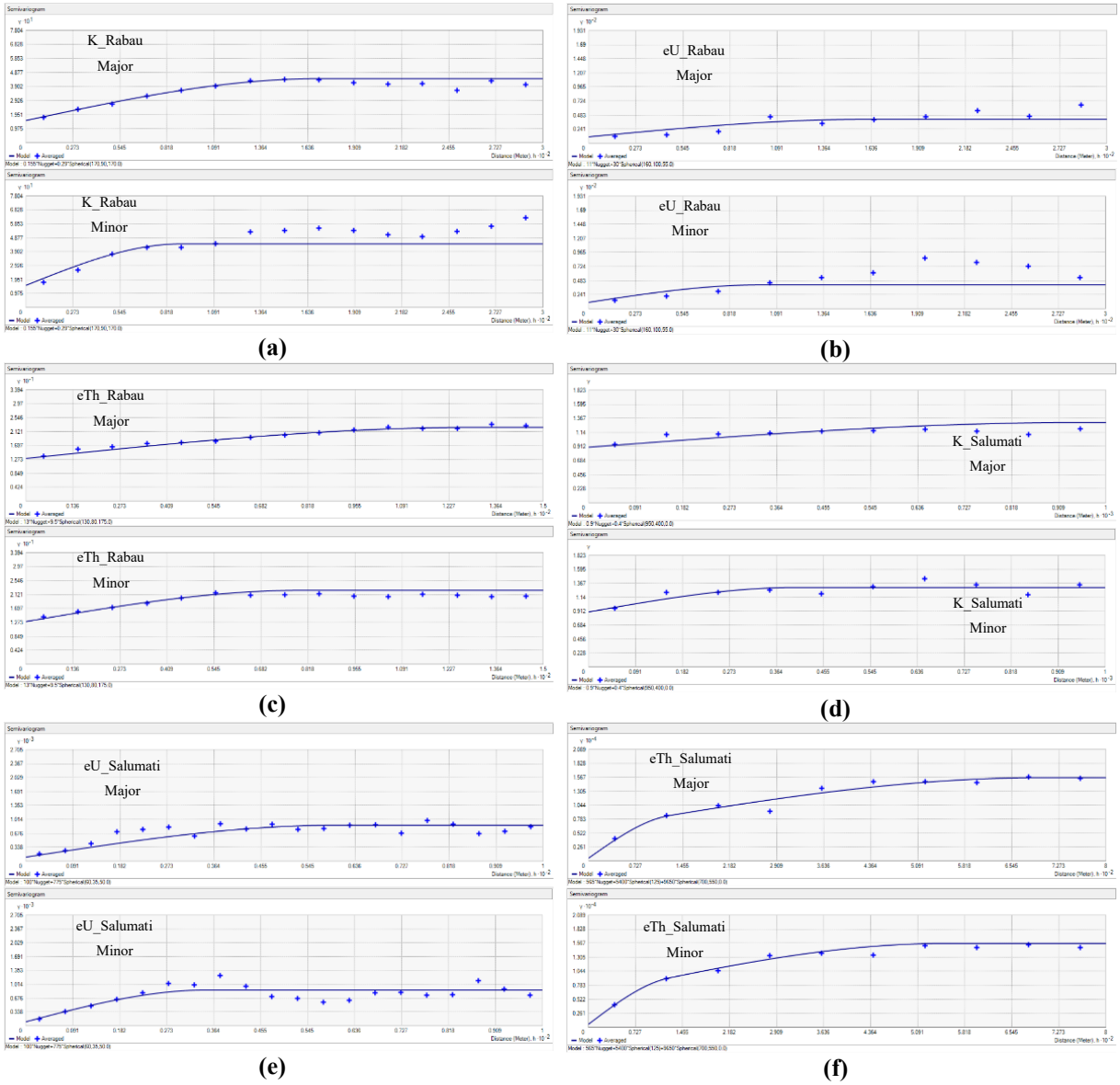

Figure 5. Variogram models of radionuclides parameter: (a) K of Rabau Sector; (b) eU of Rabau Sector; (c) eTh of Rabau Sector; (d) K of Salumati Sector; (e) eU of Salumati Sector; and (f) eTh of Salumati Sector. The blue plus sign indicates the experimental variogram, while the blue line shows the variogram model

Table 2. Validation of predicted values

Sector	Parameters	Mean Standardized Error	Root Mean Squared Standardized Error
Rabau	K	0.0001	1.0000
	eU	-0.0002	1.0450
	eTh	-0.0002	1.0220
Salumati	K	-0.0014	0.8941
	eU	0.0016	1.0986
	eTh	0.0018	1.0350

p-ISSN 0854-1418
e-ISSN 2503-426X

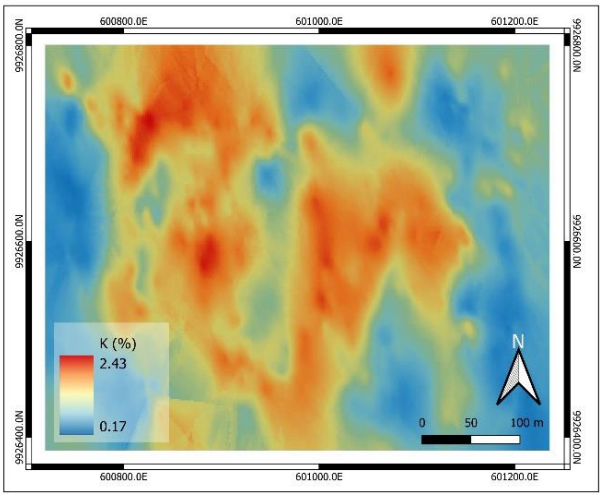

(a)

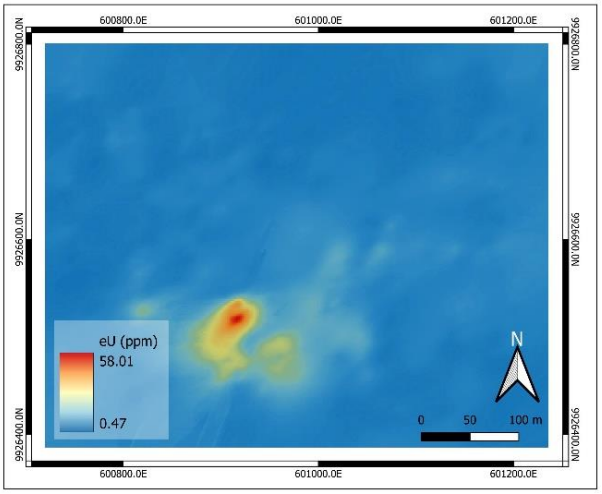

(b)

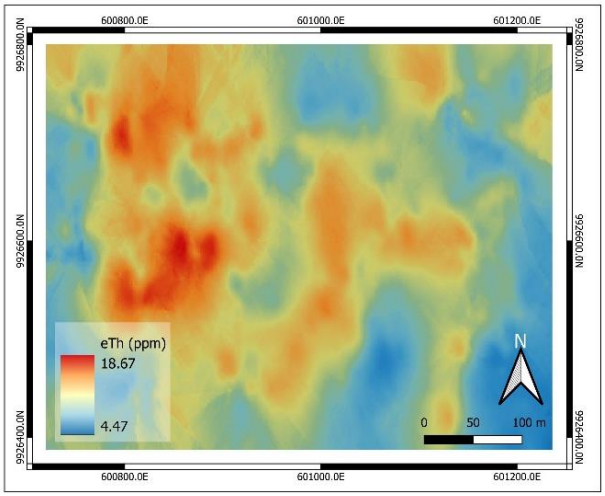

(c)

Figure 6. Estimated distribution models of Rabau Sector for K (a), eU (b), and eTh (c)

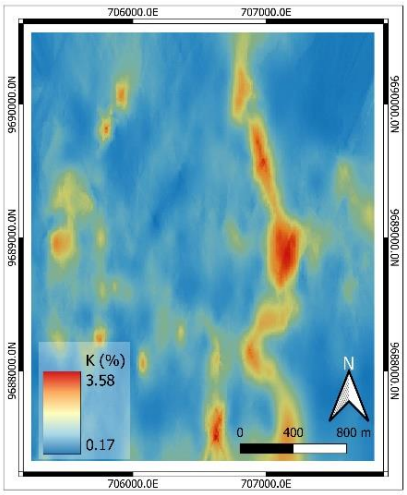

(a)

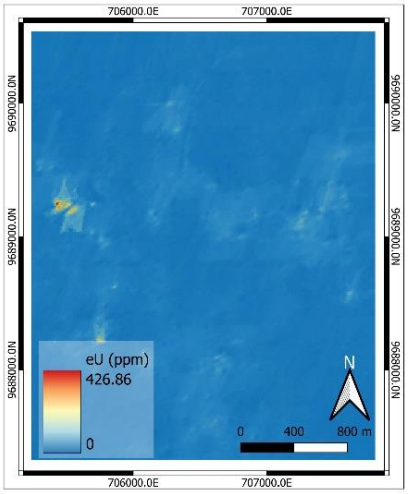

(b)

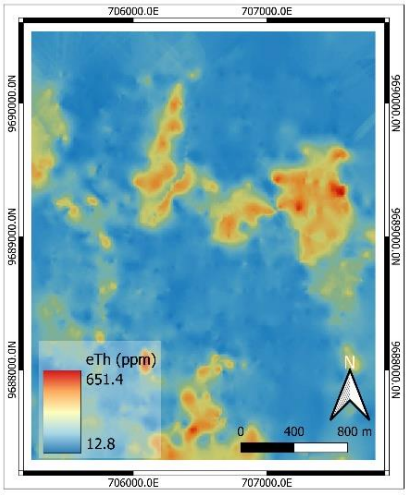

(c)

Figure 7. Estimated distribution models of Salumati Sector for K (a), eU (b), and eTh (c)

Composite Delineation

The composite ternary map of radionuclides for both the Rabau and Salumati sectors is shown in Figure 8. Distinct variations in color combinations, reflecting differences in radionuclide concentrations, are evident between the two sectors. These color variations were used to delineate the composite images into several units for further interpretation.

In the Rabau Sector, four units were identified based on radiometric contrasts (Figure 9 and Table 3). The R1 unit, characterized by an intense red hue, corresponds to zones with high eU concentration, indicating a significant radiometric anomaly and a potential target for uranium exploration. The R2 unit, with a subdued red tone, represents a transitional area containing moderate eU levels and minor contributions from K or eTh. The R3 unit shows a mixed blue-green coloration, characteristic of K and eTh dominance with minimal uranium content, likely reflecting background radiometric levels. The R4 unit, characterized by dimmed blue-green shades, indicates low overall radioelement content, particularly U, suggesting unmineralized or unaltered host rock.

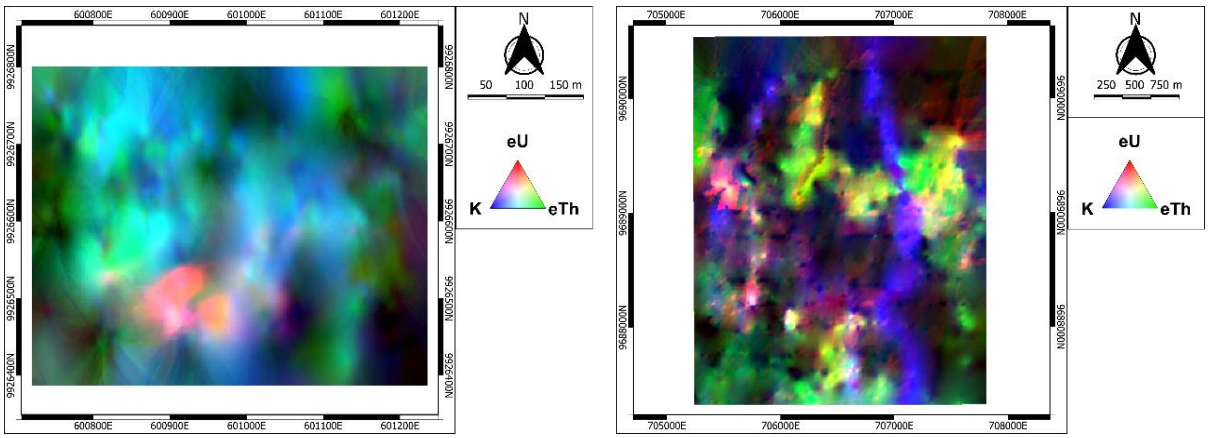

(a) **(b)**

Figure 8. The composite of all radionuclides of Rabau Sector (a) and Salumati Sector (b)

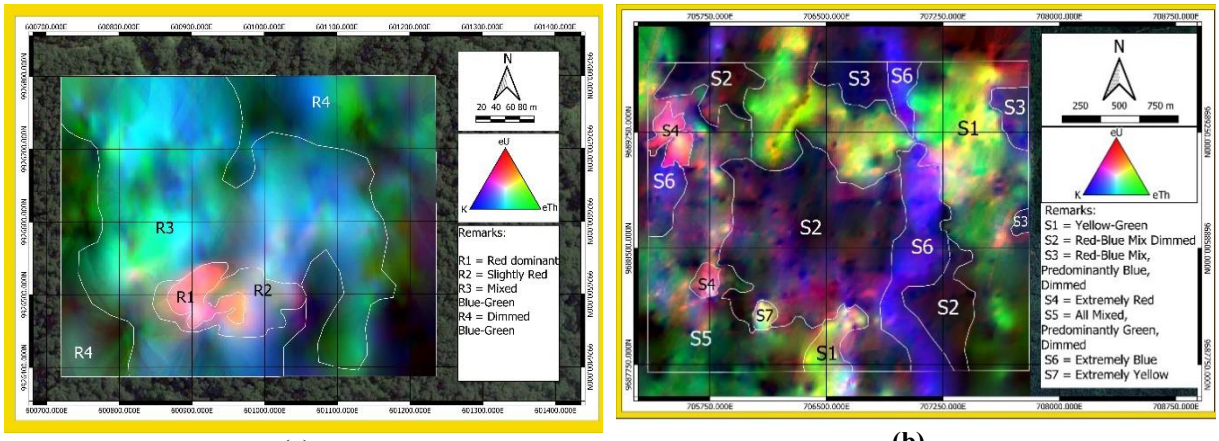

(a) **(b)**

Figure 9. The radiometric composite map delineation of Rabau Sector (a) and Salumati Sector (b)

p-ISSN 0854-1418
e-ISSN 2503-426X

Table 3. Color-coded radiometric units for Rabau and Salumati Sectors

Location	Units	Color	Identification
Rabau	R1	Red Dominant	Predominantly eU
	R2	Slightly Red	eU is dominant, but mixed with other components
	R3	Mixed Blue-Green	K and eTh are uniformly distributed at high concentrations
	R4	Dimmed Blue-Green	K and eTh are uniformly distributed at low concentrations
Salumati	S1	Yellow-Green	A mixture of eU and eTh, with eTh being more dominant, both occur at low concentrations
	S2	Red-Blue Mix Dimmed	A uniform mixture of eU and K at low concentrations
	S3	Red-Blue Mix, Predominantly Blue, Dimmed	A mixture of eU and K, with K being more dominant, both occur at low concentrations
	S4	Extremely Red	Predominantly eU
	S5	All Mixed, Predominantly Green, Dimmed	A mixture of all three components, with eTh being the most dominant, all occur at low concentrations
	S6	Extremely Blue	Predominantly K
	S7	Predominantly Yellow	A uniform mixture of eU and eTh at high concentrations

The Salumati Sector displays greater compositional diversity, with seven delineated units. The S1 unit, appearing in yellow-green tones, indicates K–eTh dominance with negligible eU. The S2 unit, characterized by a dimmed red-blue mix, suggests moderate eU and K levels but relatively low overall radiometric intensity. The S3 unit also presents a red-blue combination, with a dominant blue and dimmed, reflecting high K with lesser eU and minor eTh. In contrast, the S4 unit stands out with extremely red coloration, strongly indicating zones of very high eU enrichment. The S5 unit shows a mixture of all colors with a dominant greenish hue and dimmed intensity, pointing to moderate eTh levels with low K and eU. The S6 unit, with a bright blue tone, denotes a K-rich area. In contrast, the S7 unit, in intense yellow, represents zones with a strong combination of K and eU and minimal eTh influence.

DISCUSSION

Analysis of radiometric anisotropy reveals a consistent N–S orientation for K and eTh, aligning with the dip-direction of lithological units in the Rabau Sector [20] and the volcanic unit trend in the Salumati Sector [33]. Meanwhile, eU shows an NE–SW anisotropy, suggesting surface mobility has shifted its spatial pattern away from the lithological control seen in the more immobile K and eTh. This deviation is likely influenced by river systems, which in both sectors predominantly follow a NE–SW course. Fluvial erosion along these channels exposes outcrops and facilitates surface run-off, leaching uranium into the river. Structural controls may act indirectly by creating zones of weakness that guide river erosion. In the Rabau Sector, the observed anisotropy also differs from the subsurface orebody orientation [20], indicating a strong modification by surface processes.

The variogram model shows nugget-sill ratios ranging from 0.036 to 0.692, reflecting variable spatial dependence across the datasets. Most radionuclides in both sectors exhibit moderate spatial dependence, except for eU and eTh in the Salumati Sector, which show strong spatial dependence [34]. The highest ratio (0.692; for K in the Salumati Sector) approaches weak spatial continuity,

possibly linked to geochemical content of K, U, and Th variation in the lithology unit. Volcanic rocks in the area, particularly alkaline types, are generally richer in K than limestones. In the Salumati Sector, the close juxtaposition of volcanic rocks and limestones likely produces high K variability, contributing to the elevated nugget effect.

Comparisons between the delineated radiometric units and geological maps (Figure 10) reveal significant correlations. In the Rabau Sector (Figure 10a), the R1 and R2 units generally coincide with hornfels, indicating a relationship between high eU concentration and thermal-metamorphic rocks. Meanwhile, the R3 and R4 units correspond to metatuff and metasiltstone, showing little radiometric distinction between them. This condition is consistent with the idea that radiometric mapping is more sensitive to lithologies with differing origins than variations within the same protolith. Although hornfels, metatuff, and metasiltstone originating from the Pinoh Metamorphic Complex [17], [18], the hornfels likely experienced higher-grade contact metamorphism, making it radiometrically distinct. In contrast, the metatuff and metasiltstone have undergone similar metamorphic conditions.

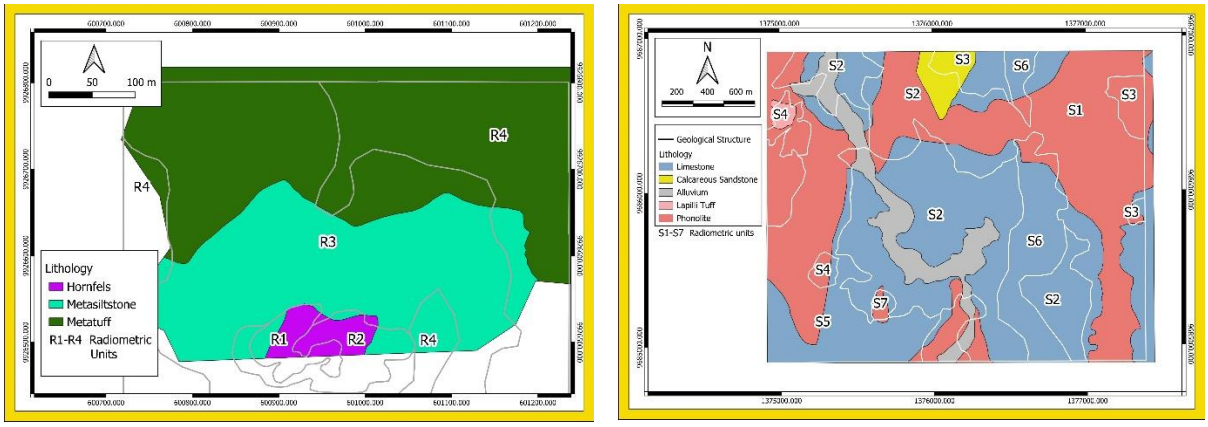

(a) (b)

Figure 10. Comparison between the delineated units from radiometric mapping and the geological maps of Rabau (a) and Salumati Sector (b).

A comparable pattern occurs in the Salumati Sector (Figure 10b). The S1, S3, S5, and S7 units correspond mainly to the phonolite, with variations in radiometric response likely reflecting compositional heterogeneity or differential alteration, particularly in thorium, possibly due to supergene enrichment [33], [35], [36]. The S4 unit coincides with the tuff and appears to delineate zones where uranium, leached from phonolites, has been adsorbed into smectite-altered zones in the tuff [33]. Its extent beyond the mapped tuff suggests it may serve as a potential proxy for alteration zoning rather than just lithological boundaries. The S2 and S6 units correspond to limestone and calcareous sandstone, with minor spatial inconsistencies. The isolated S6 unit occurrence within alluvium may indicate a lithological heterogeneity or a K-enriched sublayer in limestone. The alluvium itself is poorly resolved in the radiometric map, likely due to its heterogeneous and reworked nature, which blends the radiometric signatures of its source materials. These observations highlight that radiometric mapping is effective for

p-ISSN 0854-1418
e-ISSN 2503-426X

distinguishing lithologies with different origins or alteration histories, but is less effective in differentiating units derived from the same protolith or sedimentary environments where source material dominates by mixed-source materials.

Several related studies demonstrate the effectiveness of radiometric methods for lithological discrimination. However, the performance observed in the present work differs from several of these, likely due to contrasting climatic conditions. For instance, in an arid desert environment of Wadi Ababa, Egypt, the integration of airborne gamma-ray spectrometry with remote sensing achieved precise mapping of lithologies and uranium-bearing structures [5]. Similarly, radiometric surveys on Lipari Island in the Mediterranean successfully delineated kaolinized volcanic zones through the detection of K depletion [7]. The clarity of radiometric anomalies in such exposed terrains emphasizes the distinct challenge and significance of achieving comparable results in tropical regions such as Rabau and Salumati.

In the semi-arid Kebbi–Sokoto basement complex of northwestern Nigeria, ternary radiometric mapping distinguished between gneiss, granitoid, and migmatite [6]. This ability to discriminate lithologies of different metamorphic grades is comparable to observations in the Rabau Sector, where hornfels was radiometrically differentiated from other metasediments due to a stronger thermal overprint. Likewise, in the hyper-arid Central Eastern Desert of Egypt, airborne and ground-based radiometry effectively delineated hydrothermal alteration zones and pegmatite-hosted uranium mineralizations with high precision [9], [37], aided by continuous surface exposure. By contrast, the Salumati Sector achieved comparable differentiation of altered tuff units despite dense vegetation cover and intense tropical weathering, underscoring the role of rock alteration in generating distinctive radiometric responses [7]–[10].

In a tropical context similar to this study, uranium and thorium mapping in Bangka Island [14], [15], [38] demonstrated that thorium is more stable than uranium and potassium in weathered and reworked terrains such as alluvial and paleochannel deposits. This condition aligns with the Salumati Sector results, where thorium enrichment proved to be a reliable indicator of lithological and alteration variability.

Overall, this study advances the applicability of radiometric methods in tropical regions where intense chemical weathering and dense vegetation have traditionally posed challenges and remain underrepresented in the literature. The findings from the Rabau and Salumati Sectors confirm that gamma-ray spectrometry can effectively distinguish rock units when differences in genesis or alteration exist, even among lithologies derived from the same protolith. These findings expand the known applicability of gamma-ray spectrometry in tropical terrains. Integrating geostatistical modeling, such as ordinary kriging and anisotropy analysis, enhances the spatial reliability of radiometric data interpretation.

However, certain limitations should be acknowledged. First, the use of visual-qualitative comparison for validation introduces potential error in visual delineation. Second, both the alteration process and the lithological protolith must be considered in interpretation, as they strongly influence radiometric signatures. Third, the kriging parameter, including range selection, may affect the scalability of the generated maps, potentially overlooking smaller-scale structural controls. Despite these constraints,

the study demonstrates the interpretive value of radiometric ratios and highlights radiometric surveying as a cost-effective tool for early-stage uranium exploration in Indonesia.

CONCLUSION

Radiometric mapping in tropical environments can effectively differentiate lithologies where contrasts in genesis or alteration exist. In the Rabau Sector, elevated eU concentrations in hornfels reflect thermal metamorphism, while metatuff and metasiltstone remain indistinguishable due to their common protolith. In the Salumati Sector, eTh–eU zoning within phonolite indicates compositional heterogeneity or varying degrees of alteration, and elevated eU in altered tuff indicates uranium remobilization in smectite-rich zones. These findings demonstrate that gamma-ray spectrometry, when interpreted within a robust geological framework, is a valuable tool for early-stage uranium exploration in tropical regions of Indonesia. However, its effectiveness declines for lithologies with similar origins or reworked sediments, underscoring the need to account for the alteration process during interpretation.

ACKNOWLEDGMENT

This research was funded by a grant from the Research Organization of Nuclear Energy, BRIN (RP HITN D2473/2023). We would also like to thank Mr. Suharji and the local people of Kalan and Mamuju for their support during data acquisition.

REFERENCES

[1] M. A. El-Sadek, "Radiospectrometric and magnetic signatures of a gold mine in Egypt," *J. Appl. Geophys.*, vol. 67, no. 1, pp. 34–43, 2009, doi: 10.1016/j.jappgeo.2008.08.012.

[2] S. K. Atta, "Mapping subsurface geological structures in the Birimian Supergroup, Ghana using airborne magnetic and radiometric data: Implications for gold exploration," *J. African Earth Sci.*, vol. 205, no. June, p. 105003, 2023, doi: 10.1016/j.jafrearsci.2023.105003.

[3] K. O. Olomo, S. Bayode, O. A. Alagbe, G. M. Olayanju, and O. K. Olaleye, "Multifaceted investigation of porphyry Cu-Au-Mo deposit in hydrothermal alteration zones within the gold field of Ilesha Schist Belt," *Malaysian J. Geosci.*, vol. 6, no. 2, pp. 45–53, 2022, doi: 10.26480/mjg.02.2022.45.53.

[4] R. B. K. Shives, B. W. Charbonneau, and K. L. Ford, "The detection of potassic alteration by gamma-ray spectrometry - Recognition of alteration related to mineralization," *Geophysics*, vol. 65, no. 6, pp. 2001–2011, 2000, doi: 10.1190/1.1444884.

[5] M. A. El-Sadek and M. I. Mousa, "Integration of space images and airborne radiometric data for discrimination of radioactive mineralizations at Wadi Araba area, North Eastern Desert, Egypt," *Egypt. J. Remote Sens. Sp. Sci.*, vol. 13, no. 1, pp. 11–19, 2010, doi: 10.1016/j.ejrs.2010.07.002.

[6] J. Aisabokhae and I. Osazuwa, "Radiometric mapping and spectral based classification of rocks using remote sensing data analysis: The Precambrian basement complex, NW Nigeria," *Remote Sens. Appl. Soc. Environ.*, vol. 21, no. November 2020, 2021, doi: 10.1016/j.rsase.2020.100447.

[7] P. Chiozzi, V. Pasquale, and M. Verdoya, "Radiometric survey for exploration of hydrothermal alteration in a volcanic area," *J. Geochemical Explor.*, vol. 93, no. 1, pp. 13–20, 2007, doi: 10.1016/j.gexplo.2006.07.002.

[8] A. A. Azzazy, A. A. Elhusseiny, and S. Zamzam, "Integrated radioactive mineralization modeling using analytical hierarchy process for airborne radiometric and remote sensing data, East Wadi Qena (EWQ), Eastern Desert, Egypt," *J. Appl. Geophys.*, vol. 206, no. May, p. 104805, 2022, doi: 10.1016/j.jappgeo.2022.104805.

[9] S. O. Elkhateeb and M. A. G. Abdellatif, "Delineation potential gold mineralization zones in a part of Central Eastern Desert, Egypt using Airborne Magnetic and Radiometric data," *NRIAG J. Astron. Geophys.*, vol. 7, no. 2, pp. 361–376, 2018, doi: 10.1016/j.nrjag.2018.05.010.

p-ISSN 0854-1418
e-ISSN 2503-426X

[10] D. Richarte, S. Correa-Otto, F. Lince Klinger, and M. Giménez, "Geophysical characterization of a low sulfidation epithermal gold and silver deposit, Mendoza, Argentina," *J. South Am. Earth Sci.*, vol. 123, no. November 2022, 2023, doi: 10.1016/j.jsames.2023.104227.

[11] H. Syaeful, R. C. Ciputra, T. B. Adimedha, A. Sumaryanto, I. G. Sukadana, F. D. Indrastomo, F. Pratiwi, Sucipta, H. A. Pratama, D. Mustika, K. S. Widana, S. Widodo, M. Burhannudinnur, I. Syafri, and B. Sutopo, "Radiometric Signatures of Gold Mineralization Zone in Pongkor, West Java, Indonesia: A Baseline for Radiometric Mapping Application on Low-Sulfidation Epithermal Deposit," *Resources*, vol. 13, no. 1, 2024, doi: 10.3390/resources13010002.

[12] H. Syaeful, I. G. Sukadana, and A. Sumaryanto, "Radiometric mapping for Naturally Occurring Radioactive Materials (NORM) assessment in Mamuju, West Sulawesi," *Atom Indones.*, vol. 40, no. 1, pp. 33–39, 2014, doi: 10.17146/aij.2014.263.

[13] I. Gde Sukadana, I. Wayan Warmada, A. Harijoko, F. D. Indrastomo, and H. Syaeful, "The Application of Geostatistical Analysis on Radiometric Mapping Data to Recognized the Uranium and Thorium Anomaly in West Sulawesi, Indonesia.," *IOP Conf. Ser. Earth Environ. Sci.*, vol. 819, no. 1, 2021, doi: 10.1088/1755-1315/819/1/012030.

[14] Ngadenin, H. Syaeful, K. S. Widana, and M. Nurdin, "Potensi Thorium dan Uranium di Kabupaten Bangka Barat," *Eksplorium*, vol. 35, no. 2, pp. 69–84, 2014, [Online]. Available: https://ejournal.brin.go.id/eksplorium/article/view/8083/6196.

[15] Ngadenin, R. Fauzi, H. Syaeful, K. S. Widana, I. G. Sukadana, F. D. Indrastomo, and Widodo, "Uncovering the Distribution Zones of Uranium and Thorium in Bangka Island," *Atom Indones.*, vol. 49, no. 3, pp. 177–184, 2023, doi: 10.55981/aij.2023.1288.

[16] H. Syaeful, I. G. Sukadana, Y. S. B. Susilo, F. D. Indrastomo, A. G. Muhammad, and Ngadenin, "Uranium Exploration, Deposit and Resources: The Key of Nuclear power plant development program in Indonesia," *J. Phys. Conf. Ser.*, vol. 2048, no. 1, 2021, doi: 10.1088/1742-6596/2048/1/012003.

[17] H. T. Breitfeld, L. Davies, R. Hall, R. Armstrong, M. Foster, G. Lister, M. Thirwall, N. Grassineau, J. Hennig-Breitfeld, and M. W. A. van Hattum, "Mesozoic Paleo-Pacific Subduction Beneath SW Borneo: U-Pb Geochronology of the Schwaner Granitoids and the Pinoh Metamorphic Group," *Front. Earth Sci.*, vol. 8, no. December, 2020, doi: 10.3389/feart.2020.568715.

[18] L. Davies, R. Hall, and R. Armstrong, "Cretaceous Crust in South West Borneo: Petrological, Geochemical, and Geochronological Constraints from the Schwaner Mountains," *Proceedings of Indonesian Petroleum Association*, 2014, [Online]. Available: https://archives.datapages.com/data/ipa_pdf/2014/IPA14-G-025.htm.

[19] J. Hennig, H. T. Breitfeld, R. Hall, and A. M. S. Nugraha, "The Mesozoic Tectono-Magmatic Evolution at the Paleo-Pacific Subduction Zone in West Borneo," *Gondwana Res.*, vol. 48, pp. 292–310, 2017, doi: 10.1016/j.gr.2017.05.001.

[20] R. Ciputra, S. Suharji, D. Kamajati, and H. Syaeful, "Application of geostatistics to complete uranium resources estimation of Rabau Hulu Sector, Kalan, West Kalimantan," *E3S Web Conf.*, vol. 200, 2020, doi: 10.1051/e3sconf/202020006001.

[21] B. Sutopo, R. Witjahjati, and Y. Wusana, "Sintesis Geologi dan Mineralisasi Uranium Sektor Rabau Hulu, Kalimantan Barat," in Internal Report of PPBGN BATAN, Jakarta, 2005.

[22] Pusat Pengembangan Bahan Galian Nuklir BATAN, *Prospeksi Super Detil Sektor Rabau Kallimantan Barat Tahun 1985/1986 (Internal Report)*, Jakarta, 1986.

[23] R. Witjahjati and H. Supalal, *Perhitungan Sumber Daya Uranium di Daerah Rabau Hulu Kalimantan Barat*, in: Internal Report of PPBGN BATAN, Jakarta, 1991.

[24] I. Rosianna, E. D. Nugraha, H. Syaeful, S. Putra, M. Hosoda, N. Akata, and S. Tokonami, "Natural radioactivity of laterite and volcanic rock sample for radioactive mineral exploration in Mamuju, Indonesia," *Geosci.*, vol. 10, no. 9, pp. 1–13, 2020, doi: 10.3390/geosciences10090376.

[25] I. Rosianna, E. D. Nugraha, H Tazoe, H. Syaeful, A. G. Muhammad, I. G. Sukadana, F. D. Indrastomo, Ngadenin, F. Pratiwi, A. Sumaryanto, Sucipta, H. A. Pratama, D. Mustika, L. Nirwani, Nurokhim, Y. Omori, M. Hosoda, N. Akata, and S. Tokonami, "Uranium Isotope Characterization in Volcanic Deposits in a High Natural Background Radiation Area, Mamuju, Indonesia,"

Geosci., vol. 13, no. 12, pp. 1–13, 2023, doi: 10.3390/geosciences13120388.

[26] I. G. Sukadana, I. W. Warmada, F. Pratiwi, A. Harijoko, and T. B. Adimedha, "Elemental mapping for characterizing of thorium and Rare Earth Elements (REE) bearing minerals using μXRF," *Atom Indones.*, vol. 48, no. 2, pp. 87–98, 2022, doi: 10.17146/aij.2022.1215.

[27] R. Hall, I. R. Cloke, S. Nur'aini, S. D. Puspita, S. J. Calvert, and C. F. Elders, "The North Makassar Straits: What lies beneath?," *Pet. Geosci*., vol. 15, no. 2, pp. 147–158, 2009, doi: 10.1144/1354-079309-829.

[28] S. Bergman, D. Q. Coffield, J. P. Talbot, and R. Garrard, "Tertiary Tectonic and magmatic evolution of western Sulawesi and the Makassar Strait, Indonesia: Evidence for a Miocene continent-continent collision," *Geol. Soc. London Spec. Publ*., vol. 106, pp. 391–429, 1996, doi: 10.1144/GSL.SP.1996.106.01.25.

[29] A. Guntoro, "The formation of the Makassar Strait and the separation between SE Kalimantan and SW Sulawesi," *Journal of Asian Earth Sciences*, vol. 17, no. 1-2, pp. 79–98, 1999, doi: 10.1016/S0743-9547(98)00037-3.

[30] W. A. Draniswari, S. I. T. Kusuma, T. B. Adimedha, and I. G. Sukadana, "Peran Kontaminasi Kerak pada Diferensiasi Magma Pembentuk Batuan Vulkanik Sungai Ampalas, Mamuju, Sulawesi Barat," *Eksplorium*, vol. 41, no. 2, p. 73, 2020, doi: 10.17146/eksplorium.2020.41.2.6040.

[31] I. G. Sukadana, A. Harijoko, and L. D. Setidjadji, "Tataan Tektonika Batuan Gunung Api Di Komplek Adang, Kabupaten Mamuju, Propinsi Sulawesi Barat," Eksplorium, vol. 36, no. 1, pp. 31–44, 2015, doi: 10.17146/eksplorium.2015.36.1.2771.

[32] F. D. Indrastomo, I. G. Sukadana, A. Saepuloh, A. H. Harsolumakso, and D. Kamajati, "Interpretasi Vulkanostratigrafi Daerah Mamuju Berdasarkan Analisis Citra Landsat-8," Eksplorium, vol. 36, no. 2, p. 71, 2015, doi: 10.17146/eksplorium.2015.36.2.2772.

[33] H. E. Wulan, *Studi Alterasi Hidrotermal dan Pengayaan Unsur Radioaktif di Daerah Takandeang, Tapalang, Mamuju, Sulawesi Barat*, Universitas Gadjah Mada, 2020.

[34] C. A. Cambardella, T. B. Moorman, J. M. Novak, T. B. Parkin, D. L. Karlen, R. F. Turco, and A. E. Konopka, "Field-Scale Variability of Soil Properties in Central Iowa Soils," *Soil Sci. Soc. Am. J.*, vol. 58, no. 5, pp. 1501–1511, 1994, doi: 10.2136/sssaj1994.03615995005800050033x.

[35] I. G. Sukadana, F. D. Indrastomo, and Ngadenin, "Sebaran Alterasi Batuan Berdasarkan Rasio Th/U di Tapalang, mamuju, Sulawesi Barat," Ris.Geo.Tam, vol. 28, no. 2, pp. 141–155, 2018, doi: 10.14203/risetgeotam2018.v28.661.

[36] I. G. Sukadana, Sulaeman, H. Syaeful, F. D. Indrastomo, T. B. Adimedha, R. C. Ciputra, F. Pratiwi, D. Mustika, A. Sumaryanto, M. Burhannudinnur, R. A. P. Rijanti, P. Santosa, and S. Widodo, "High Field Strength Element (HFSE) and Rare Earth Element (REE) Enrichment in Laterite Deposit of High Background Natural Radiation Area (HBNRA) of Mamuju, West Sulawesi, Indonesia," *Resources*, vol. 14 no. 5: 84, pp. 1–23, 2025, doi: 10.3390/resources14050084.

[37] M. H. M. Yousef, "Delineation of radiometric anomalies and conductive zones using gamma-ray spectrometric and electromagnetic methods, east Gabal El-Urf area, Northern Eastern Desert, Egypt," *Appl. Radiat. Isot*., vol. 153, no. April, p. 108822, 2019, doi: 10.1016/j.apradiso.2019.108822.

[38] Ngadenin, I. G. Sukadana, A.G. Muhammad, F. D. Indrastomo, I. Rosianna, R. C. Ciputra, T. B. Adimedha, F. Pratiwi, and Y. Rachael, "Radioactive Mineral Distribution on Tin Placer Deposits of Southeast Asia Tin Belt Granite in Bangka Island," *Eksplorium*, vol. 44, no. 2, p. 49, 2024, doi: 10.55981/eksplorium.2023.6969.